Tower Grounding Improvement Versus Line Surge Arresters: Comparison of Remedial Measures for High-BFOR Subtransmission Lines

Fabio Massimo Gatta, Alberto Geri, Stefano Lauria, *Member, IEEE*, Marco Maccioni, and Francesco Palone

***Abstract*—This paper presents a technical/economic comparison between remedial measures aimed at improving the lightning performance of an existing Italian three-phase 150-kV overhead line. The line is characterized by a very high back-flashover rate (BFOR), due to large grounding resistance values. Two countermeasures are proposed: grounding system improvement with additional vertical rods and line metal oxide surge arrester (MOSA) installation on one or all phases. A Monte Carlo ATP-EMTP procedure developed by the authors, which takes into account both the tower grounding nonlinear transient response due to soil ionization and MOSA nonlinear response, has been applied to evaluate and compare the effectiveness of the proposed countermeasures. The installation of MOSA on all phases is technically the best option, but it is relatively expensive. Tower grounding improvement and MOSA installation on the lower phase yield very similar BFORs: the economic comparison strongly depends on tower's accessibility and soil nature.**

***Index Terms*—ATP-EMTP, back-flashover rate (BFOR), grounding system, high-voltage (HV) overhead line, metal oxide surge arrester (MOSA), Monte Carlo method.**

I. Introduction

In Italy, 132- or 150-kV high-voltage (HV) overhead lines (OHLs) form the bulk (40 000 km) of Terna's (the Italian transmission network operator, TSO) subtransmission networks, often running through hilly or mountainous terrain due to the country's geography. The attendant increased exposure to lightning, in conjunction with the relatively high keraunic level of mainland Italy, is liable to cause undesirably high back-flashover rates (BFORs). This notably applies to older lines, whose tower grounding systems can be also impaired by corrosion [1], sometimes leading to equivalent grounding resistances in excess of 100 Ω. High BFORs are often associated to a limited number of "rogue" towers, characterized by a combination of high lightning exposure (e.g., located on ridges or mountainsides) and high grounding resistance. A straightforward corrective measure is tower grounding improvement, which can range from total rebuilding of badly corroded systems to more limited actions, such as the installation of a few (2–4) additional rods alongside the existing grounding system. In recent years, lightweight polymer-insulated metal oxide surge arresters (MOSAs), so-called "line arresters," have been installed on OHL towers directly across phase insulation [2]–[4]. In Italy, where tower grounding improvement often incurs serious delays due to the legal/regulatory framework (authorization and property expropriation problems), the installation of surge arresters meets less obstacles under this regard and can constitute an alternative solution to the rogue towers problem.

This paper presents a technical–economic comparison of the aforementioned BFOR countermeasures for an existing 150-kV subtransmission OHL operated by Terna in Center Italy. The 10.8-km-long line crosses a mountain ridge with a moderate keraunic level (3.5 flashes/km^2/year) for Italy, whereas soil resistivity is about 1000 Ω · m; furthermore, grounding resistance has substantially increased at some towers due to corrosion of earth electrodes. All these factors contribute to an exceptionally high BFOR recorded by the TSO (about 70 faults/100 km/year).

Both applicable countermeasures, that is, grounding system improvement with additional vertical rods and line arrester installation on one or more phases, are investigated by means of ATP-EMTP transient simulations. The impact of line arresters on the lightning performance of OHLs has been the object of several papers: deterministic studies, basically focused on arrester location and using ATP-EMTP transient simulations, are presented in [5] and [6]. A mixed Monte-Carlo–deterministic procedure was proposed in [7], whereas a probabilistic approach (not using Monte Carlo method) is detailed in [8], in order to evaluate the failure risk of surge arresters caused by lightning flash. Despite different approaches, all aforementioned studies point out to the highly beneficial role played by line arresters (whose systematic installation can reduce or even nullify the BFOR), as well as discussing the effectiveness of partial protection by line surge arrester (only one phase per tower and/or only some towers). In this paper, the lightning performance of the line, in the starting configuration and after the implementation of either of the proposed countermeasures, is evaluated by means of a Monte Carlo ATP-EMTP procedure [9], [10] developed by the authors and able, in addition to

Manuscript received December 31, 2014; revised April 7, 2015; accepted June 14, 2015. Paper 2014-PSEC-0853.R1, approved for publication in the IEEE Transactions on Industry Applications by the Power Systems Engineering Committee of the IEEE Industry Applications Society.

F. M. Gatta, A. Geri, S. Lauria, and M. Maccioni are with the Department of Astronautics, Electrical and Energetics Engineering (DIAEE), University of Rome "La Sapienza," 00185 Rome, Italy (e-mail: fabiomassimo.gatta@uniroma1.it; alberto.geri@uniroma1.it; stefano.lauria@uniroma1.it; marco.maccioni@uniroma1.it).

F. Palone is with Terna Rete Italia S.p.A., 00156 Rome, Italy (e-mail: francesco.palone@terna.it).

Digital Object Identifier 10.1109/TIA.2015.2448613

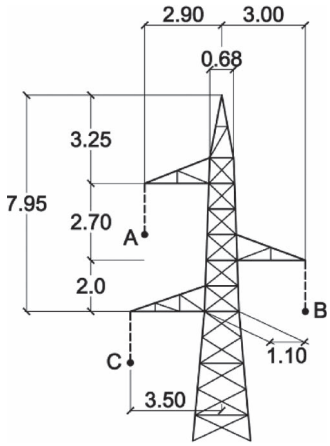

Fig. 1. Outline of the OHL tower head (dimensions are in meters).

TABLE I
PHASE AND SHIELD WIRE CONDUCTOR COORDINATES

	A	B	C	SW
x (m)	−2.9	3	−3.5	0
y (m)	22.1	20.1	18.1	27.7

previous contributions, to provide a statistical assessment of MOSA failure rates. Detailed modeling of line insulation, tower grounding nonlinear transient response due to soil ionization, and MOSAs, where present, is included. Results obtained are finally analyzed and compared, both from a technical and from an economic point of view.

II. System Modeling Details

A. OHL Model

The single-circuit three-phase 150-kV 50-Hz OHL under study is 10.8 km long (37 line spans, for an average 290-m span length), with a single 11.5-mm steel ground wire and the phases, equipped with ~~single 31.5-mm aluminium conductor steel reinforced conductors~~, in a triangular arrangement, as shown in Fig. 1. The simulated tower height is 27.7 m (the average tower height of the 38 towers), with an 11.4-m phase conductor sag and a 9.7-m shield wire sag. Table I reports the phase and shield wire conductors coordinates. All line spans were simulated in ATP-EMTP by means of the "JMarti" frequency-dependent model (reference frequency for modal calculation taken at 500 kHz). At both ends of the simulated line stretch, the OHL model is connected to the line surge impedances: phase conductors are then terminated on a three-phase 150-kV 50-Hz voltage system, with one of the phases always at the maximum operating voltage to ground (i.e., $170 \cdot \sqrt{2}/\sqrt{3}$ kV), whereas the shield wire is solidly grounded. Segments and crossarms of the OHL towers have been simulated by means of lossless single-phase transmission lines (Bergeron model, with $Z_T = 200\ \Omega$); at each tower, the shield wire is connected to the tower peak. Corona effect was not simulated.

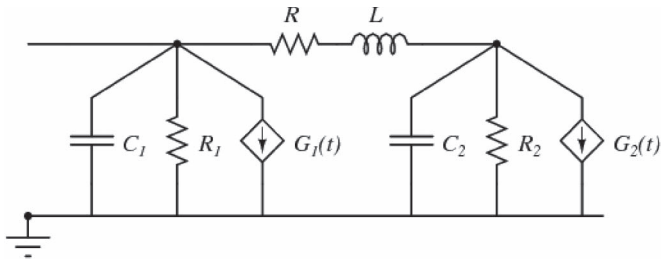

Fig. 2. Simplified pi-circuit model of tower grounding system [7]–[9].

B. Line Insulation Model

Line insulation breakdown has been simulated with the CIGRE Leader Progression Model, implemented with ATP-EMTP by means of the embedded "MODELS" programming/simulation language, i.e.,

$$\frac{dl}{dt} = k \cdot u(t) \left[\frac{u(t)}{d_G - l(t)} - E_0 \right] \quad (1)$$

where $l(t)$ (m) is the leader length, d_G (m) is the gap length, and $u(t)$ (kV) is the voltage across the gap. E_0 (kV/m) and k ($\mathrm{m}^2 \cdot \mathrm{kV}^{-2} \cdot \mathrm{s}^{-1}$) depend on gap configuration and impulse polarity. The gap length d_G is 1.46 m.

C. Lightning Model

The well-known "Heidler" impulse current source available in ATP-EMTP has been used in all simulations, i.e.,

$$i(t) = \frac{I_P}{\eta} \cdot \frac{k_s^n}{1 + k_s^n} \cdot e^{-\frac{t}{\tau_2}} \quad (2)$$

where I_P is the peak current; η is the correction factor of the peak current; $k_s = t/\tau_1$; τ_1 and τ_2 are time constants determining current rise time and decay time, respectively; and n is the current steepness factor.

D. Grounding System Model

The transient simulation of tower grounding systems is carried out by means of the simplified pi-circuit model proposed by the authors in [11]–[13] and depicted in Fig. 2.

The pi-circuit model is obtained by synthesis of a full circuit model [14], able to reproduce the transient impedance of extended grounding systems also taking into account the soil ionization. The linear components of the pi circuit (shunt resistors and capacitors R_1, R_2, C_1, and C_2; longitudinal resistor and inductance R and L) are estimated by comparing the input impedances of the full circuit model (ATP-EMTP frequency scans without considering ionization) and of the pi circuit, switching off the ideal voltage-controlled current sources G_1 and G_2. A μGA-based [15] optimization procedure minimizes the standard deviation between the input impedances in the frequency range 1 Hz to 1 MHz. Ideal voltage-controlled current sources G_1 and G_2 simulate nonlinear soil ionization caused

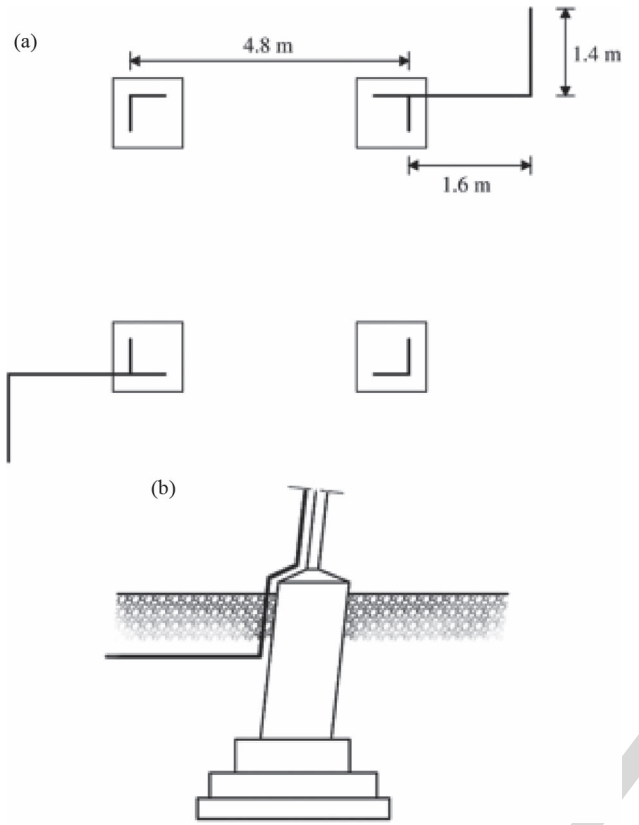

Fig. 3. (a) Sketch of the MT1 grounding system. (b) Connection at the tower foot (burying depth 0.8 m).

by large current pulses. The analytical functions assigned to G_1 and G_2 are $(i = 1, 2)$

$$G_i(t) = \frac{V_{Ri}(t)}{F_i(t)} - \frac{V_{Ri}(t)}{R_i} \tag{3}$$

being $V_{Ri}(t)$ the instantaneous value of the voltage across the linear shunt resistor R_i, and $F_i(t)$ is given by

$$F_i(t) = R_i - \alpha_i \cdot \log\left(10^{-4} + \beta_i \frac{V_{R_i}(t)}{R_i}\right), \quad F_i \in [10^{-4}; R_i] \tag{4}$$

where α_i (expressed in ohms) and β_i (expressed in A^{-1}) take into account nonlinear soil ionization phenomena. The pi-circuit model is implemented with ATP-EMTP by means of the "MODELS" programming language [16].

Thirty-five out of 38 towers of the line under study are equipped with the simplest Terna's standard tower grounding system, code-named MT1 and depicted in Fig. 3. The low-frequency ground resistance value of the simulated MT1 grounding system is 114 Ω (considering a constant 1000-Ω · m soil resistivity value along the whole line), which is in accordance with ground resistance values measured at 50 Hz by the TSO, ranging from 50 to 125 Ω. At the remaining three towers, the measured ground resistance at 50 Hz is about 500 Ω: such a large value is very probably due to corrosion of the original grounding system. In the simulations, a 2-m-long vertical rod (1ROD in the following), with a low-frequency ground resistance value around 500 Ω, is used.

TABLE II
LINEAR PARAMETER VALUES FOR PI-TYPE SIMPLIFIED EQUIVALENT CIRCUITS

	R_1 (Ω)	R_2 (Ω)	R (Ω)	L (μH)	C_1 (nF)	C_2 (nF)
MT1	386.8	8.2	153.9	1.0	2.74	1.00
1ROD	928.9	119.9	972.6	0.48	0.09	0.79
4RODS‖1ROD	96.2	25.6	196.9	3.9	4.70	0.33
4RODS‖MT1	60.2	748.9	5.1	25.0	4.97	0.57

TABLE III
NONLINEAR COEFFICIENT VALUES FOR PI-TYPE SIMPLIFIED EQUIVALENT CIRCUITS

	α_1 (Ω)	α_2 (Ω)	β_1 (A^{-1})	β_2 (A^{-1})
MT1	27.08	0	48.08	1.50
1ROD	44.00	20.00	4010.6	8500.5
4RODS‖1ROD	2.96	2.91	4010.6	8500.5
4RODS‖MT1	1.41	0.91	3950.2	7458.5

As reported in Section I, one of the foreseeable countermeasures aimed at improving the grounding system behavior is the addition of vertical rods: in this paper, four vertical rods, each 5 m long and connected to one tower foot, are simulated (Countermeasure 1 in the following). The addition of four vertical rods to the preexisting MT1 grounding system (4RODS‖MT1 in the following) decreases the low-frequency ground resistance value from 114 Ω to about 56 Ω, whereas the same addition to 1ROD configuration (4RODS‖1ROD in the following) causes a very large ground resistance decrease from 500 to 67 Ω.

Numerical values of the pi-circuit parameters used to simulate the above-described grounding system configurations are reported in Tables II and III.

E. MOSA Model

MOSAs have been simulated with the model described in [17] and depicted in Fig. 4, consisting of a constant resistance $R = 1$ mΩ, two nonlinear resistors A_0 and A_1, whose $V-I$ characteristics (both of the form $I = BV^q$) are determined by the parameters listed in Table IV, and the inductances L_0 and L_1 defined by the following equations (values are in microhenries):

$$L_0 = \frac{1}{12} \cdot \frac{V_{r1/T_2} - V_{r8/20}}{V_{r8/20}} \cdot V_n \tag{5}$$

$$L_1 = \frac{1}{4} \cdot \frac{V_{r1/T_2} - V_{r8/20}}{V_{r8/20}} \cdot V_n \tag{6}$$

where V_n is the arrester rated voltage, $V_{r1/T2}$ is the residual voltage for a 10-kA fast front current surge $(1/T_2\ \mu\mathrm{s})$, and

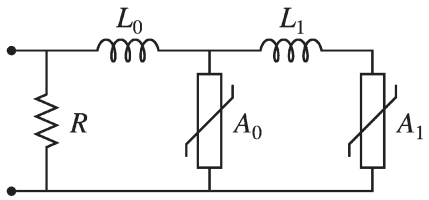

Fig. 4. MOSA model used in simulations [13].

TABLE IV
$V-I$ CHARACTERISTICS FOR A_0 AND A_1
(VALUES ARE IN P.U. OF THE $V_{R8/20}$ VOLTAGE)

I (kA)	A_0 (p.u.)	A_1 (p.u.)
$2{\cdot}10^{-6}$	0.810	0.623
0.1	0.974	0.788
1	1.052	0.866
3	1.108	0.922
10	1.195	1.009
20	1.277	1.091

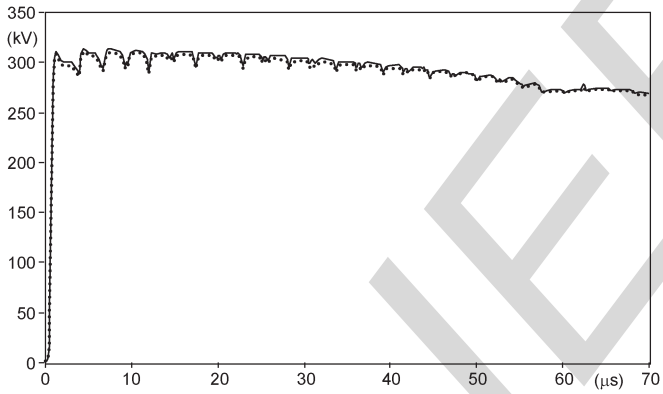

Fig. 5. Residual voltage calculated by ATP-EMTP for a 100-kA 1.46-/390-μs direct stroke. (Continuous line) MOSA simulated by true nonlinear resistance. (Dotted line) MOSA simulated by piecewise-linear resistance.

$V_{r8/20}$ is the residual voltage for a 10-kA current surge with an ~~8-/20-~~μs shape. The model is derived from the one recommended by the IEEE W.G. 3.4.11 [18], but parameters are directly calculated by using the standard data reported in the arrester data sheets, and any iterative procedure in order to correct parameter values is needed. The model has been validated by comparison between the calculated residual voltages and those reported on manufacturer's data sheet [17] and by experimental tests [19].

The ATP-EMTP implementation of the model may be performed by using Type-92 branch cards [16], either the so-called true nonlinear exponential MOSA $R(i)$ or the piecewise-linear resistance $R(i)$. Fig. 5 reports the residual voltages calculated by ATP-EMTP, simulating a direct lightning (100-kA Heidler source) on a 150-kV OHL tower equipped with MOSAs on all phases, by using the two different Type-92 implementations: a very good agreement is obtained. In our Monte Carlo simulations, however, the piecewise-linear resistance Type-92 has been implemented, in order to avoid numerical oscillations observed in our complete OHL ATP-EMTP model if MOSAs are simulated with true nonlinear resistance and very large lightning strokes (peak current greater than 200 kA) hit the line.

In this paper, the installation of MOSAs along the whole OHL under study is proposed (Countermeasure 2 in the following). In the simulations described in Section IV, MOSAs are installed on each phase of the OHL ("MOSA-ABC" configuration) or only on one phase ("MOSA-A", "MOSA-B," and "MOSA-C" configurations, respectively). The simulated line arrester manufacturer's data are as follows: arrester rated voltage $U_r = 138$ kV, $V_{r1/T2} = 327$ kV, $V_{r8/20} = 313$ kV, yielding $L_0 = 0.527$ μH and $L_1 = 1.58$ μH; the MOSA's thermal energy rating $W_{\rm th}$ [20] is 345 kJ.

III. BFOR CALCULATION PROCEDURE

The BFOR is evaluated by means of a Monte Carlo procedure. A large population of $N_{\rm tot}$ lightnings, assumed to fall within a 1-km-wide swath centered on the OHL, is generated; only strokes to tower are considered, and among these, the sample of $N_{\rm Lin}$ flashes that actually hit the line is extracted by means of the Eriksson electrogeometric model [21]. The attendant strokes are simulated by means of an ATP-EMTP system model, in order to investigate the occurrence of back flashover: $N_{\rm BFO}$ total flashovers are then yielded out of N strokes. At the end of the procedure, when $N = N_{\rm tot}$, the BFOR (referred to 100 km of ~~line year~~) is then calculated as

$$\text{BFOR} = k_{\rm BFO} \cdot \frac{N_{\rm BFO}}{N_{\rm tot}} \cdot N_g \cdot 100 \qquad (7)$$

where N_g is the ground flash density (flashes/km^2/year), and $k_{\rm BFO}$ is a numerical multiplicative coefficient taking into account the percentage of the $N_{\rm Lin}$ lightning strokes, which are able to cause back flashover. In previous papers by the authors [9], [10], $k_{\rm BFO}$ was set equal to 0.6, since strokes to the shield wire (40% of the total, according to [22]) were disregarded, i.e., it is assumed that only strokes to tower are liable to cause back flashover. In the OHL under study, this assumption is not correct, due to the very high values of tower grounding resistance found along the line; thus, an approach able to roughly estimate $k_{\rm BFO}$ has been developed by the authors.

1) Evaluate the minimum peak current $I_{\rm Pmin}$ out of $N_{\rm BFO}$ lightning strokes, liable to cause back flashover.
2) For strokes to the shield wire, the minimum current liable to cause back flashover, i.e., $I_{\rm Pmin}(l)$, may be evaluated, disregarding the surge attenuation along the span, as linearly increasing from $I_{\rm Pmin}$ (stroke to tower) to $2 \cdot I_{\rm Pmin}$ (stroke to midspan).
3) Evaluate the probability $p_{\rm sw}(l)$ that a lightning stroke having I_P greater or equal to $I_{\rm Pmin}(l)$ hit the shield wire at the distance l from the tower.

TABLE V
STATISTICAL PARAMETERS OF LIGHTNING CURRENT
(FIRST NEGATIVE AND POSITIVE RETURN STROKES)

Parameter	Median value		Standard deviation	
	+	−	+	−
I_P	35 kA	31.1 kA	1.21	0.48
t_F	22 μs	3.83 μs	1.23	0.55
t_T	230 μs	77.5 μs	1.33	0.58

TABLE VI
STATISTICAL PARAMETERS FOR LINE INSULATION

Polarity	Median value (kV/m)	Standard deviation (kV/m)
+	560	16.80
−	605	18.15

4) Evaluate the integral of $p_{\rm sw}(l)$ along the shield wire, obtaining the probability $p_{\rm SW}$ referred to lightning strokes within the span able to cause back flashover.
5) Calculate $k_{\rm BFO}$ as $k_{\rm BFO} = 0.6 + 0.4 \cdot p_{\rm SW}$.

The description of the statistical inputs is given in the following subsections.

A. Lightning Polarity

Assuming that 90% of flashes to ground are negative [23], lightning polarity is associated to a random variable uniformly distributed between 0 and 1: if the random number exceeds 0.9, the flash is positive; otherwise, it is negative.

B. Lightning Stroke Parameters

The statistical variation of lightning stroke parameters (peak current I_P, front time t_F, and tail time t_T) has been assumed to follow a log-normal distribution. According to [23], values of medians and standard deviations, both for positive (+) and first negative (−) strokes, are reported in Table V.

C. Line Insulation Parameters

Statistical data for the critical field E_0 in (1), i.e., median value E_{0m} and standard deviation, are taken from [24] and summarized in Table VI. Values of constant k in (1) are $1.2 \cdot 10^{-6}$ and $1.3 \cdot 10^{-6}$ for positive and negative polarities, respectively [23].

D. Phase Angle of the Supply Voltage

The phase angle of the three-phase positive phase sequence system of impressed voltages is assumed as a uniformly distributed variable between 0% and 360%.

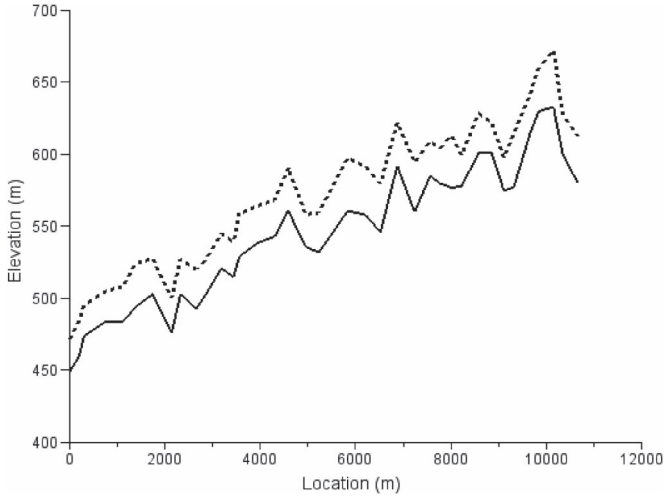

Fig. 6. (Continuous line) Ground-level height profile along the OHL. (Dotted line) Shield wire height.

E. Lightning Location

To check the occurrence of a lightning stroke to the OHL, the position of the lightning in a 1-km-wide strip, centered on the OHL (implicitly, its initial distance from the line, assuming a vertical channel), is generated as a random uniformly distributed variable, according to [25]. From the peak current value of the given lightning stroke, the attractive radius R_a of the OHL, according to Eriksson's electrogeometric model [21], is calculated as

$$R_a = 0.67 \cdot H^{0.6} \cdot I_P^{0.74} \tag{8}$$

H being the tower height (m), and I_P the peak current (kA): if the initial lightning position falls within the attractive radius of the line, then the sampled lightning is assumed to hit the OHL.

Equation (8) strictly applies to OHLs on flat terrain, which is not the case of the OHL under study (the line is built on hills, with the altitude profile shown in Fig. 6). In order to adapt (8) to an OHL not built on a flat terrain, the following simplifying assumption has been assumed: the line is considered on flat terrain, and the tower height is given by the average altitude of the OHL (572.27 m) minus the hill height at the abscissa $x = 0$ m (449 m), thus yielding $H = 132.27$ m.

IV. RESULTS

The OHL length is $L = 10.8$ km, of which $L_1 = 10.2$ km (Stretch 1, 94.4% of the OHL length) is equipped with the MT1 grounding system configuration, and $L_2 = 0.6$ km (Stretch 2, 5.6% of the OHL length) is equipped with the 1ROD grounding system configuration. The BFOR of the line, experienced by the TSO, is about 70 faults/100 km/year, being $N_g = 3.5$ flashes/km^2/year. In order to evaluate the BFOR related to each stretch of the OHL, the Monte Carlo procedure generated $N_{\rm tot} = 314\,254$ lightnings, corresponding to $N_{\rm Lin} = 100\,000$ strokes to tower.

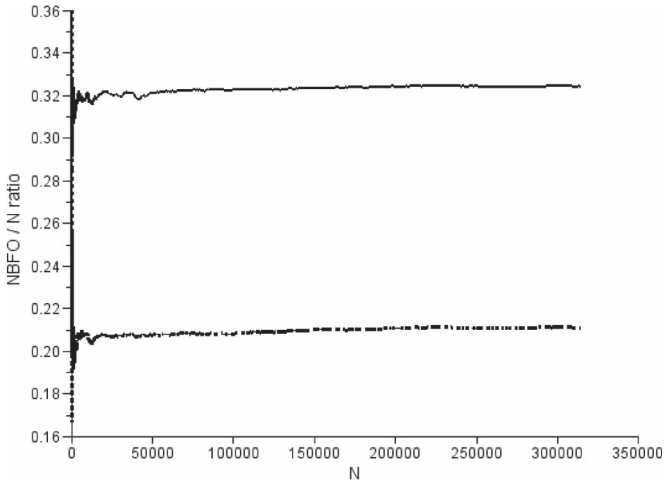

Fig. 7. Monte Carlo procedure N_{BFO}/N ratio versus N calculated for the base case configuration. (Dotted line) Stretch 1 (with MT1 grounding system). (Continuous line) Stretch 2 (with 1ROD grounding system).

TABLE VII
BFOR VALUES COMPUTED FOR THE BASE CASE CONFIGURATION

	k_{BFO}	N_{BFO}/N_{tot}	*BFOR (faults/100 km-year)*
Stretch 1	0.825	0.2112	57.600
Stretch 2	0.986	0.3243	6.216

The procedure runs in parallel on a 12 CPU cluster: the computation time of a single ATP-EMTP lightning stroke simulation is small (about 3 s), thus obtaining, for the 100 000 strokes to tower, a total computation time of about 7 h.

A. Base Case Configuration

Fig. 7 shows the plot of the N_{BFO}/N ratio versus N for each stretch of the OHL, whereas Table VII reports the corresponding BFORs evaluated by the Monte Carlo procedure. The overall BFOR is therefore about 63.8 faults/100 km/year, which is very close to the exact BFOR of the OHL (the procedure underestimates the BFOR by about 8.9%). This result thus confirms the effectiveness of the procedure and the approximations discussed and assumed in Section III in order to simulate the studied OHL. Moreover, this also shows that, despite the prominently higher N_{BFO}/N ratio of Stretch 2, the BFOR of the studied OHL is strongly dependent on the lightning performance of Stretch 1, which is very much longer than Stretch 2.

B. Countermeasure 1

As described in Section II-D, Countermeasure 1 consists in the addition of four vertical rods, each 5 m long and connected to one tower foot, to all preexisting tower grounding systems. This solution has been chosen because of its effectiveness in decreasing the low frequency values of grounding resistance, as well as for its simplicity both from a technical (civil works are not long and difficult) and from a legal/regulatory (there is no need for expropriations or widening the right of way) point of view. Table VIII reports BFORs calculated by the Monte Carlo procedure for the two stretches of the OHL, yielding an overall BFOR of about 31.58 faults/100 km/year.

TABLE VIII
BFOR VALUES COMPUTED FOR COUNTERMEASURE 1

	k_{BFO}	N_{BFO}/N_{tot}	*BFOR (faults/100 km-year)*
Stretch 1 (4RODS||MT1)	0.665	0.1334	29.339
Stretch 2 (4RODS||1ROD)	0.746	0.1549	2.244

TABLE IX
BFOR VALUES COMPUTED FOR COUNTERMEASURE 2 (MOSA-ABC CONFIGURATION)

	k_{BFO}	N_{BFO}/N_{tot}	*BFOR (faults/100 km-year)*
Stretch 1 (MOSA−ABC)	0.6	0.0	0.0
Stretch 2 (MOSA−ABC)	0.6	0.0	0.0

TABLE X
MOSAFR VALUES COMPUTED FOR COUNTERMEASURE 2 (MOSA-ABC CONFIGURATION)

	k_{MOSAF}	N_{MOSAF}/N_{tot}	*MOSAFR (failures/100 km-year)*
Stretch 1 (MOSA−ABC)	0.6	0.175	0.347
Stretch 2 (MOSA−ABC)	0.6	0.504	0.059

This result shows that Countermeasure 1 improves the lightning performance of the line and causes a 50.5% overall reduction in the BFOR; the reduction is a little more marked in Stretch 2 (about 63.9%) than in Stretch 1 (about 49.1%).

C. Countermeasure 2

As described in Section II-E, Countermeasure 2 consists in the installation of MOSAs on all OHL towers, directly across phase insulation. The Monte Carlo procedure also allows estimating the MOSA failure rate (here abbreviated as MOSAFR, expressed in failures/100 km/year) caused by an energy absorption exceeding the rated value $W_{\mathrm{th}} = 345$ kJ. The calculation is performed by replacing in (7) k_{BFO} with k_{MOSAF} (the percentage of the N_{Lin} lightnings that may cause MOSA failures) and N_{BFO} with N_{MOSAF} (number of MOSA failures). At first, the MOSA-ABC configuration (MOSAs installed on all phases) has been evaluated: Tables IX and X report the BFORs and MOSAFRs, estimated for each stretch of the line, respectively. As expected, the overall BFOR of the OHL becomes nil, whereas the overall estimated MOSAFR amounts to about 0.406 failures/100 km/year, i.e., about 0.044 failures/year (a MOSA failure every 22.7 years) in the studied OHL. Finally,

TABLE XI
BFOR VALUES COMPUTED FOR COUNTERMEASURE 2
(MOSA-A, MOSA-B, AND MOSA-C CONFIGURATIONS)

	k_{BFO}	N_{BFO}/N_{tot}	*BFOR (faults/100 km-year)*
Stretch 1 (MOSA−A)	0.762	0.1302	32.798
Stretch 2 (MOSA−A)	0.982	0.3418	6.526
Stretch 1 (MOSA−B)	0.762	0.1299	32.717
Stretch 2 (MOSA−B)	0.982	0.3410	6.511
Stretch 1 (MOSA−C)	0.751	0.1147	28.463
Stretch 2 (MOSA−C)	0.980	0.3011	5.730

TABLE XII
MOSAFR VALUES COMPUTED FOR COUNTERMEASURE 2
(MOSA-A, MOSA-B, AND MOSA-C CONFIGURATIONS)

	k_{MOSAF}	N_{MOSAF}/N_{tot}	*MOSAFR (failures/100 km-year)*
Stretch 1 (MOSA−A)	0.6	0.1075	0.213
Stretch 2 (MOSA−A)	0.6	0.3741	0.044
Stretch 1 (MOSA−B)	0.6	0.1460	0.290
Stretch 2 (MOSA−B)	0.6	0.508	0.059
Stretch 1 (MOSA−C)	0.6	0.1500	0.298
Stretch 2 (MOSA−C)	0.6	0.5220	0.061

Tables XI and XII report the BFORs and MOSAFRs obtained considering MOSA-A, MOSA-B, and MOSA-C configurations, respectively.

With regard to BFOR reduction, MOSA-C (MOSAs installed only on lower phase) is the most effective configuration (a 46.4% reduction with respect to the Base Case), whereas in terms of MOSAFR, the MOSA-A configuration yields the best results (0.257 failures/100 km/year, corresponding to 0.028 failures/year, i.e., a MOSA failure every 36 years).

D. Comparison Between Countermeasures

With regard to BFOR reduction, the best solution is the MOSA-ABC configuration of Countermeasure 2, which altogether suppresses back flashovers and only introduces a negligible MOSA failure rate (a failure every 22.7 years). However, this countermeasure is also relatively expensive, since it requires the installation of 114 MOSAs, i.e., 10.7 MOSAs/km.

The MOSA-C configuration (arresters on the lower phase) practically halves the original BFOR, at one third of the arresters' procurement cost (around 2 ~~k/unit~~ for bulk purchases).

Installation costs of Countermeasure 2 can be estimated as follows, assuming use of internal workforce (workforce is deployed in four-man squads, with a conventional cost of ~~35 /~~ man-hour):

- MOSA-C: (4 h to reach the tower + 2.5 h to install one MOSA)$\times 4 = 26$ man-hours $= 910$ €/tower; total cost for 38 towers is 110.58 k€;
- MOSA-ABC: (4 h to reach the tower + 4 h to install three MOSAs)$\times 4 = 32$ man-hours $= 1120$ €/tower; total cost for 38 towers is 270.56 k€ (it can be readily seen that labor cost is a fraction of MOSA cost).

Countermeasure 1 seems to be the most effective one from a technical–economic point of view, yielding BFOR values comparable with those of the MOSA-C configuration. Attendant civil works only involve the existing pylon base area, thus minimizing the authorization and property expropriation problems related to the substitution of the old grounding systems along the line. The cost of Countermeasure 1 strongly depends on tower location and soil hardness. In case of soft soil, costs are expected to be significantly lower than for Countermeasure 2. Considering 600 ~~/tower~~ for the grounding rods and 30 man-hours per tower, the cost of Countermeasure 1 is 1.65 ~~k/tower~~, i.e., 62.7 ~~k~~ total. Hard soil requires a vertical drilling rig, which must be leased and then, at inaccessible tower sites, also delivered by helicopter. The additional costs involved can be roughly estimated at 1500 ~~/tower~~, raising the total to 119.7 ~~k~~; in such cases, MOSA-C Countermeasure 2 becomes competitive.

V. CONCLUSION

The analysis of remedial measures aimed at reducing the exceptionally high BFOR (70 faults/100 km/year) of an existing 10.8-km-long 150-kV OHL has been carried out by means of a Monte Carlo procedure, based on detailed ATP-EMTP transient simulations. The proposed remedial measures are as follows:

1) reduction of tower grounding low-frequency resistances by installing additional vertical grounding rods;
2) installation of MOSAs across the insulation of one or all phases (line arresters).

The extensive statistically based ATP-EMTP transient analysis evidenced the following main results.

- The installation of MOSAs across all phases is the technical best, as it suppresses the BFOR, with a fairly low MOSA failure rate (a failure every 22.7 years). The capital cost of the 114 line arresters is, however, significant.
- The installation of only one arrester per tower yields a significant BFOR reduction at a lower capital cost; the most effective location is the lower phase (BFOR is 34.2 faults/100 km/year).

- The installation at each tower of four additional vertical grounding rods, each 5 m long, is comparable with the use of one MOSA per tower (lower phase), with a calculated BFOR equal to 31.6 faults/100 km/year; its economic convenience, however, depends on accessibility, as well as soil hardness, of the tower foot. An economic analysis thus requires taking into account the exact location of each tower.

As an additional remark, the study showed the applicability of the authors' ATP-EMTP Monte Carlo procedure to a practical problem.

REFERENCES

[1] S. Rajan and S. I. Venugopalan, "Corrosion and grounding systems," *IEEE Trans. Ind. Appl.*, vol. IA-13, no. 4, pp. 297–306, Jul./Aug. 1977.

[2] J. He, R. Zeng, J. Hu, S. M. Chen, and J. Zhao, "Design and application of line surge arresters to improve lightning protection characteristics of transmission lines," in *Proc. IEEE Power Eng. Soc. Transmiss. Distrib. Conf.*, 2008, pp. 1–8.

[3] S. Furukawa, O. Usuda, T. Isozaki, and T. Irie, "Development and application of lightning arresters for transmission lines," *IEEE Trans. Power Del.*, vol. 4, no. 4, pp. 2121–2129, Oct. 1989.

[4] L. M. Mswane and C. T. Gaunt, "Lightning performance improvement of the Swaziland electricity board transmission system (66 kV & 132 kV lines)—Results of the pilot project," in *Proc. IEEE Power Eng. Soc. Inaugural Conf. Expo.*, 2005, pp. 364–370.

[5] K. Munukutla, V. Vittal, G. T. Heydt, D. Chipman, and B. Keel, "A practical evaluation of surge arrester placement for transmission line lightning protection," *IEEE Trans. Power Del.*, vol. 25, no. 3, pp. 1742–1748, Jul. 2010.

[6] S. Bedoui, A. Bayadi, and A. M. Haddad, "Analysis of lightning protection with transmission line arrester using ATP/EMTP: Case of an HV 220 kV double circuit line," in *Proc. UPEC*, 2010, pp. 1–6.

[7] J. A. Martinez and F. Castro-Aranda, "Lightning flashover rate of an overhead transmission line protected by surge arresters," in *Proc. IEEE Power Eng. Soc. Gen. Meet.*, 2007, pp. 1–6.

[8] R. Shariatinasab, F. Ajri, and H. Daman-Khorshid, "Probabilistic evaluation of failure risk of transmission line surge arresters caused by lightning flash," *IET Gen., Transmiss. Distrib.*, vol. 8, no. 2, pp. 193–202, Feb. 2014.

[9] F. M. Gatta, A. Geri, S. Lauria, M. Maccioni, and A. Santarpia, "An ATP-EMTP Monte Carlo procedure for backflashover rate evaluation," in *Proc. ICLP*, 2012, pp. 1–6.

[10] F. M. Gatta, A. Geri, S. Lauria, M. Maccioni, and A. Santarpia, "An ATP-EMTP Monte Carlo procedure for backflashover rate evaluation: A comparison with the CIGRE method," *Elect. Power Syst. Res.*, vol. 113, pp. 134–140, Aug. 2014.

[11] F. M. Gatta, A. Geri, S. Lauria, and M. Maccioni, "Equivalent lumped parameter π-network of typical tower grounding systems for linear and nonlinear transient analyses," in *Proc. IEEE PowerTech Conf.*, 2009, pp. 1–6.

[12] F. M. Gatta, A. Geri, S. Lauria, and M. Maccioni, "Simplified HV tower grounding system model for backflashover simulation," in *Proc. ICLP*, 2010, pp. 1–6.

[13] F. M. Gatta, A. Geri, S. Lauria, and M. Maccioni, "Simplified HV tower grounding system model for backflashover simulation," *Elect. Power Syst. Res.*, vol. 85, pp. 16–23, Apr. 2012.

[14] A. Geri, "Behavior of grounding systems excited by high impulse currents: The model and its validation," *IEEE Trans. Power Del.*, vol. 14, no. 3, pp. 1008–1017, Jul. 1999.

[15] D. L. Carroll, FORTRAN Genetic Algorithm (GA) Driver. [Online]. Available: http://cuaerospace.com/carroll/ga.html

[16] Alternative Transients Program (ATP) Rule Book, Canadian/American EMTP User Group, Linn, OR, USA, 1995.

[17] P. Pinceti and M. Giannettoni, "A simplified model for zinc oxide surge arresters," *IEEE Trans. Power Del.*, vol. 14, no. 2, pp. 393–398, Apr. 1999.

[18] IEEE Working Group 3.4.11, "Modeling of metal oxide surge arresters," *IEEE Trans. Power Del.*, vol. 7, no. 1, pp. 302–309, Jan. 1992.

[19] C. A. Christodoulou, F. A. Assimakopoulou, I. F. Gonos, and I. A. Stathopulos, "Simulation of metal oxide surge arresters behavior," in *Proc. IEEE Power Electron. Spec. Conf.*, 2008, pp. 1862–1866.

[20] *Surge Arresters—Part 4: Metal-Oxide Surge Arresters Without Gaps for A.C. Systems*, IEC 60099-4 ed. 3.0, Jun. 2014.

[21] A. J. Eriksson, "An improved electrogeometric model for transmission line shielding analysis," *IEEE Trans. Power Del.*, vol. 2, no. 3, pp. 871–886, Jul. 1987.

[22] A. R. Hileman, *Insulation Coordination for Power Systems*. New York, NY, USA: Marcel Dekker, 1999.

[23] CIGRE Working Group 01 of SC 33, "Guide to Procedures for Estimating the Lightning Performance of Transmission Lines," GRE Brochure no. 63, Oct. 1991.

[24] Lightning and Insulator Subcommittee of the T&D Committee, "Parameters of lightning strokes: A review," *IEEE Trans. Power Del.*, vol. 20, no. 1, pp. 346–358, Jan. 2005.

[25] J. A. Martinez and F. Castro-Aranda, "Lightning performance analysis of overhead transmission lines using the EMTP," *IEEE Trans. Power Del.*, vol. 20, no. 3, pp. 2200–2210, Jul. 2005.

Fabio Massimo Gatta was born in Alatri, Italy, in 1956. He received the M.Sc.(Hons.) degree in electrical engineering from the University of Rome "La Sapienza," Rome, Italy, in 1981.

He then joined the Department of Astronautics, Electrical and Energy Engineering of the University of Rome "La Sapienza," where he became a Researcher in 1985 and was appointed an Associate Professor of electrical power systems in 1998. His main research interests are in the field of power system analysis; long-distance transmission; transient stability; temporary and transient overvoltages; series and shunt compensation; ~~SSR~~; distributed generation; power plants; design, planning~~,~~ and operation of transmission and distribution networks; ~~and~~ unconventional distribution systems. AQ3

Alberto Geri was born in Terni, Italy, on August 4, 1961. He received the M.Sc. degree in electrical engineering from the University of Rome "La Sapienza," Rome, Italy, in 1987.

He began his academic activity in 1989 as a Researcher of Electrical Science with the University of Rome "La Sapienza," where he was an Associate Professor of electrical engineering from 2000 to 2015 and has been an Associate Professor of electrical power systems since 2015. He has been a recipient of many research contracts and grants from institutional sources and private investors. He began his research activity in 1982. He has authored or coauthored over 150 papers presented at international conferences or published in peer-reviewed international journals. His interests include direct electrical energy conversion by magnetohydrodynamics devices, renewable energy conversion and bioremediation by microbial fuel cells, low-frequency electric and magnetic field computation, high-frequency magnetic device modeling, nonlinear electromagnetic problems in power systems related to lightning, medium-voltage/low-voltage distribution networks, distributed generation, and smart and micro grids.

Prof. Geri is a corresponding member of the International Council on Large Electric Systems (CIGRÉ) Working Group C4.406 "Performance of Grounding Electrodes for Lightning Currents."

Stefano Lauria (M'98) was born in Rome, Italy, in 1969. He received the M.Sc. and Ph.D. degrees in electrical engineering from the University of Rome "La Sapienza," Rome, in 1996 and 2001, respectively.

In 2000, he joined the Department of Astronautics, Electrical and Energy Engineering of the University of Rome "La Sapienza" as a Researcher. His research interests include power systems analysis, distributed generation, HV and extra HV ac cable transmission, shunt compensation, and electromagnetic transients. He has authored or coauthored over 85 papers presented at international conferences or published in peer-reviewed international journals.

Dr. Lauria is a member of the International Council on Large Electric Systems (CIGRÉ) and the IEEE Power and Energy Society.

Marco Maccioni was born in Anagni, Italy, on June 24, 1978. He received the M.Sc. and Ph.D. degrees in electrical engineering from the University of Rome "La Sapienza," Rome, Italy, in 2005 and 2010, respectively.

He is currently with the Department of Astronautics, Electrical and Energetics Engineering of the University of Rome "La Sapienza" on a research grant. His main interests include power system analysis, evolutionary algorithms implemented on parallel architectures and applied to solve synthesis problems and/or multiobjective optimization problems, smart grids, and nonlinear electromagnetic problems related to lightning.

Francesco Palone was born in Rome, Italy, in 1985. He received the B.Sc., M.Sc., and Ph.D. degrees from the University of Rome "La Sapienza," Rome, Italy, in 2007, 2009, and 2013, respectively, all in electrical engineering.

In 2009, he joined the Engineering Department, Terna, Rome, the Italian transmission system operator and network owner, engaging in electromagnetic transient studies, transformer specification, and battery energy storage design. Since 2012, he has been with Terna Rete Italia S.p.A, Rome. His fields of research are cable and transformer modeling for time- and frequency-domain studies, compensation apparatus (reactors, phase-shifting transformers, synchronous condensers), and interconnection lines.

AUTHOR QUERIES

AUTHOR PLEASE ANSWER ALL QUERIES

AQ1 = ACSR was expanded as "aluminium conductor steel reinforced." Please check if appropriate. Otherwise, please provide the corresponding expanded form.
AQ2 = The value "1 Hz ÷ 1 MHz" was changed to "1 Hz to 1 MHz. " Please check if appropriate. Otherwise, please make the necessary changes.
AQ3 = Please provide the expanded form of "SSR."

END OF ALL QUERIES